

Synthesis, Structure, and Reactivity of Sodium (η^5 -Cyclopentadienyl)nitrosylcobaltate

Wayne P. Weiner, Frederick J. Hollander, and Robert G. Bergman*

Contribution from the Department of Chemistry, University of California, Berkeley, California 94720. Received April 26, 1984

Abstract: Treatment of $(\text{CpCoNO})_2$ with Na/Hg in Et_2O results in the formation of NaCpCoNO (**1**). Similarly, NaMeCpCoNO was prepared and metathesized with PPNCl to form $[\text{PPN}][\text{MeCpCoNO}]$. The structure of the novel, low-valent nitrosyl metalate was determined by X-ray diffraction, and the results of this study show that the nitrosyl ligand is linear. Treatment of **1** with R_3SnCl ($\text{R} = \text{Me}, \text{Ph}$) affords the new complexes $\text{CpCo}(\text{NO})\text{SnR}_3$, and similarly, the reaction of **1** with Ph_2SnCl_2 forms the trinuclear complex $\text{Ph}_2\text{Sn}(\text{CpCoNO})_2$. IR spectroscopy indicates that these Co-Sn complexes each contain linear, three-electron-donating nitrosyl ligands. The dinuclear complexes $\text{Cp}_2\text{CoCr}(\text{NO})_3$ (**5**) and $\text{Cp}_2\text{CoMn}(\text{NO})_2\text{PMe}_3$ (**6**) are formed by treatment of **1** with $\text{CpCo}(\text{NO})_2\text{Cl}$ and $[\text{CpMn}(\text{CO})(\text{NO})\text{PMe}_3]\text{BF}_4$, respectively. Complexes **5** and **6** represent rare examples of heteronuclear bridging nitrosyl dimers. The structure of **6** was determined by X-ray diffraction. The results of this study revealed that the bridging nitrosyl ligands are symmetrical with respect to the metal centers.

Introduction

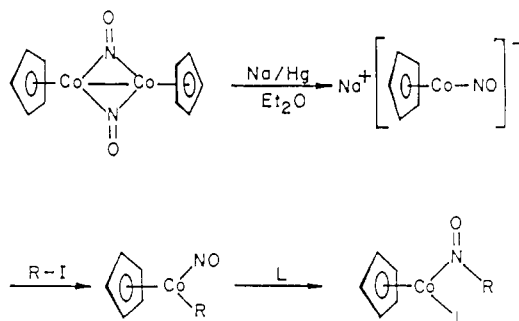
The extensive studies focused on transition-metal anions reflect in part the increasing practical and theoretical interest in nucleophilic reactions of these species with organic, main-group, and transition-metal electrophiles. One example is the successive alkylation of $\text{Na}_2\text{Fe}(\text{CO})_4$, which results in the high-yield formation of ketones via CO migratory insertion and reductive elimination steps.^{1a} Another is the chemistry of the unique highly reduced species studied recently by Ellis and co-workers.^{1b,c}

Despite this interest, the large majority of transition-metal anions presently known contain CO ligands; i.e., they are members of the carbonyl metalate class. In contrast, very few examples of low-valent nitrosyl metalates are known. Recently, we reported the synthesis of a novel nitrosyl metalate, $\text{Na}[(\eta^5\text{-C}_5\text{H}_5)\text{CoNO}]$ (**1**), characterized by spectroscopic data.² This anion was shown to react cleanly with alkyl halides to form the corresponding alkyl nitrosyl complexes. These complexes underwent facile NO migratory insertion to yield coordinatively unsaturated nitrosoalkane complexes, which were trapped by triphenylphosphine (Scheme I). Stimulated by a general interest in transition-metal-mediated carbon-nitrogen bond formation and by the unique formulation of **1** as a rare, low-valent transition-metal nitrosyl anion,³ we have investigated the structure of the methylcyclopentadienyl derivative of **1** by X-ray diffraction. In addition to the results of this study, we wish to report on the reactivity of **1** with organometallic substrates, which have resulted in the synthesis and characterization of several novel organotransition-metal nitrosyl complexes.

Results and Discussion

Synthesis and X-ray Diffraction Analysis of $[\text{PPN}][\text{MeCpCoNO}]$. The neutral diamagnetic nitrosylcobalt dimer $[\text{CpCoNO}]_2$ was reduced with Na/Hg in ether as described earlier,² resulting in the precipitation of $\text{Na}[\text{CpCoNO}]$ (**1**) as a pink, highly pyrophoric solid. This material was identified on the basis of a single cyclopentadienyl resonance in the ^1H NMR spectrum (CD_3CN) at δ 4.2 and a low-frequency M-NO stretch in CH_3CN at 1560 cm^{-1} . Similarly, $\text{Na}[\text{MeCpCoNO}]$ (**1a**) can be obtained from the reduction of $(\text{MeCpCoNO})_2$ and displays a M-NO stretch in

Scheme I



CH_3CN at 1580 cm^{-1} . Both sodium salts can be metathesized with bis(triphenylphosphine)nitrogen(1+) chloride (PPNCl). The resulting PPN salts can be recrystallized from 5:1 $\text{CH}_2\text{Cl}_2/\text{CH}_3\text{CN}$ at -40°C to form moderately air-stable crystals. Analytical and ^1H NMR spectroscopic data revealed these salts to contain 0.6 and 1.0 mol of acetonitrile of solvation for the Cp and MeCp complexes, respectively. Crystals of **1a** were selected for the X-ray diffraction analysis due to their increased stability and ease of handling relative to the parent $\text{PPN}^+\text{1}$ salt.

Large orange-red crystals of $\text{PPN}^+\text{1a}$ were obtained by slow recrystallization from 4:1 $\text{Et}_2\text{O}/\text{CH}_3\text{CN}$. The structure of this complex was solved and refined to a final R value of 3.09%. An ORTEP drawing of the $(\text{MeCpCoNO})^-$ fragment is presented in Figure 1, with important bond distances and angles listed in the caption. The PPN cation and the acetonitrile of solvation have been omitted for clarity; in the cation the P-N-P angle of 145° and all of the remaining bond distances and angles are unexceptional.^{3a} The structure consists of well-separated anions, cations, and acetonitrile molecules. Specifically, there are no strong interactions between the anion and acetonitrile molecule (see stereoview of unit cell in Figure 2).

This study represents the first example of a structurally characterized cyclopentadienyl transition-metal nitrosyl anion and is particularly unique in that no other back-bonding ligands (e.g., CO, CN) are attached to the metal center.³ One important feature of the structure is the linear metal nitrosyl bonding mode, with a Co-N-O angle of 176° . This implies three-electron donation by a nitrosonium ligand,^{4a} placing cobalt in the formal -1 oxidation state. The lack of directly analogous complexes makes it difficult

(1) (a) Collman, J. P. *Acc. Chem. Res.* **1975**, *8*, 342. (b) See, for example: Chen, Y.-S.; Ellis, J. E. *J. Am. Chem. Soc.* **1983**, *105*, 1689. (c) Lin, J. T.; Ellis, J. E. *Ibid.* **1983**, *105*, 6252 and earlier papers.

(2) Weiner, W. P.; Bergman, R. G. *J. Am. Chem. Soc.* **1983**, *105*, 3922.

(3) For examples of other low-valent nitrosylmetalates, see: (a) Dannell, K. H.; Chen, Y.; Belknap, K.; Wu, C. C.; Bernal, I.; Creswick, M. W.; Huang, H. N. *Inorg. Chem.* **1983**, *22*, 418. (b) Steimann, M.; Nagel, U.; Grenz, R.; Beck, W. *J. Organomet. Chem.* **1983**, *247*, 171. (c) Stevens, R. E.; Gladfelter, W. L. *Inorg. Chem.* **1983**, *22*, 2034. (d) Müller, A.; Eltzner, W.; Sarkar, S.; Bögge, H.; Aymonino, P. J.; Mohan, N.; Seyer, U.; Subramanian, P. Z. *Anorg. Allg. Chem.* **1983**, *503*, 22. (e) Fjare, K. L.; Ellis, J. E. *J. Am. Chem. Soc.* **1983**, *105*, 2303. The salts in ref 3a-d have been characterized by X-ray diffraction.

(4) (a) Collman, J. P.; Hegedus, L. S. "Principles and Applications of Organotransition Metal Chemistry", University Science Books: Mill Valley, CA, 1980; p 145. (b) Feltham, R. D.; Enemark, J. H. *Top. Inorg. Stereochem.* **1981**, *12*, 155. (c) Ronova, I. A.; Alekseeva, N. V.; Veniaminov, N. N.; Kravets, M. A. *Zh. Strukt. Khim.* **1975**, *16*, 476. (d) Cox, A. P.; Brittain, A. H. *Trans. Faraday Soc.* **1970**, *66*, 557.

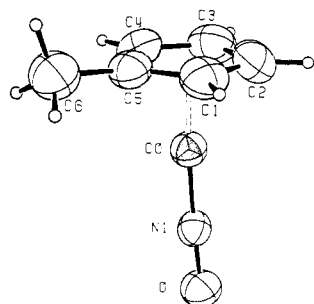


Figure 1. ORTEP drawing of **1a**: Co-N(1) = 1.590 (2) Å, Co-Cp = 1.710 Å, N(1)-O = 1.229 (2) Å, C(6)-C(5) = 1.474 (4) Å, N(1)-Co-Cp = 176.4°, and Co-N-O = 176.16°.

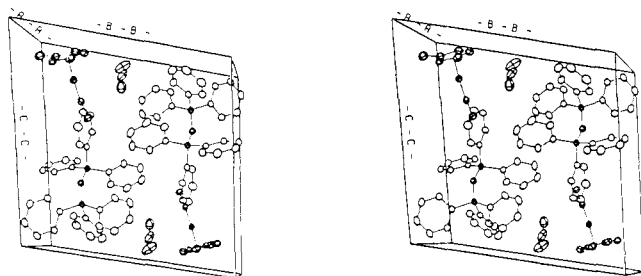


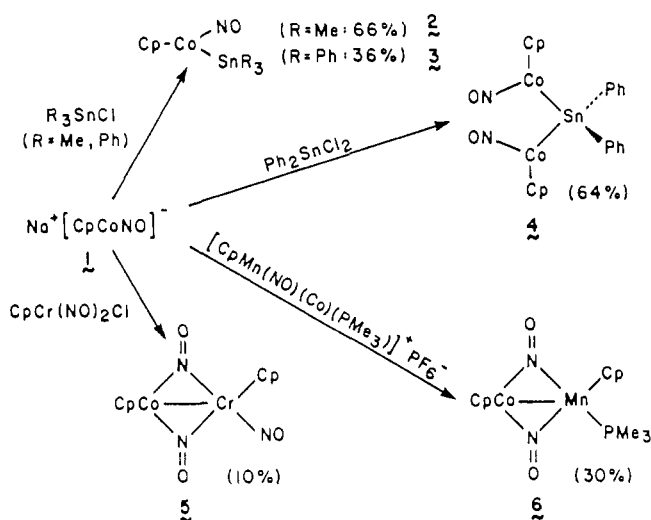
Figure 2. Stereoview of the unit cell of **1a**.

to settle on "normal" structural parameters with which to compare the Co-N bond length of 1.59 Å. In addition, comparison is complicated by the fact that known M-N and N-O bond lengths are quite variable from system to system in both anionic and neutral metal nitrosyls. M-N distances are reported^{4b} as short as 1.65 Å, and some are longer than 2.0 Å; N-O distances range from 1.02 to 1.27 Å.

Perhaps the closest analogue to $[\text{MeCpCoNO}]^-$ is the neutral isoelectronic nickel complex CpNiNO . This material is a liquid at room temperature, and although it solidifies on cooling, apparently no X-ray structural data on it are available. The nickel complex has been examined by electron diffraction and microwave spectroscopy; there is reasonable, although not perfect, agreement in the bond lengths determined in the two most recent studies.^{4c,d} Comparison of these values ($d_{\text{Ni-N}} = 1.58, 1.63$ Å; $d_{\text{N-O}} = 1.16, 1.17$ Å) with those for cobalt anion **1a** ($d_{\text{Co-N}} = 1.59$ Å; $d_{\text{N-O}} = 1.23$ Å) reveal very similar C-N lengths, and a longer N-O bond in the anionic cobalt complex. The N-O difference is consistent with donation of negative charge from the metal center to the nitrosyl ligand. Comparison of N-O stretching frequencies in the infrared spectra of these complexes also supports this picture. The N-O stretching vibration for CpNiNO is at 1809 cm^{-1} ; this is strongly shifted to 1560 and 1580 cm^{-1} for cobalt anions **1** and **1a** in acetonitrile solvent, where contact-ion pairing should be minimal. In comparison with organic systems, the N-O bond in **1a** at 1.23 Å is considerably shorter than the N-O single bond of 1.34 Å found in glyoxime ($\text{HON}=\text{CHCH}=\text{NOH}$)⁵, but longer than the NO double-bond length of 1.19 Å found in the monomeric aliphatic nitrosoalkane (+)-10-bromo-2-chloro-2-nitroso-camphane.⁶ The presumed partial double bond character of the N-O linkage is consistent with the back-bonding character of the nitrosyl ligand.^{4a}

Chemistry of $[\text{Na}[\text{CpCoNO}]]$ (1**).** Treatment of THF solutions of the parent nitrosyl anion **1** with trimethyl- or triphenyltin chloride resulted in the smooth formation of the corresponding dinuclear cobalt-tin complexes **2** and **3** (Scheme II). The trimethyltin complex **2** was isolated in 66% yield as an analytically pure, air-sensitive, viscous red oil after the solvent was vacuum transferred from the filtered reaction mixture. It exhibits an M-NO stretch at 1775 cm^{-1} (THF); this complex is now neutral,

Scheme II



and so the N-O frequency has returned to a more normal region of the spectrum, closer to the 1809 cm^{-1} value observed for CpNiNO . Tin complex **2** also exhibits two singlets in the ^1H NMR spectrum in C_6D_6 at δ 4.5 and 0.8 in the ratio of 5:9. The triphenyltin complex **3** was isolated as air-stable brown crystals in 36% yield by recrystallization of the crude reaction mixture from 3:1 toluene/pentane at -40°C . The ^1H NMR spectrum (CD_3CN) of **3** displays, in addition to the aromatic resonances, a single Cp signal at δ 4.4, and a M-NO stretch (THF) at 1775 cm^{-1} . Similarly, the trinuclear complex **4** was prepared in 64% yield by the reaction of **1** with diphenyltin dichloride and isolated as dark red needles by recrystallization of the crude reaction product from pentane. Upon warming to room temperature, the crystals began to melt, forming an air-sensitive waxy solid. The IR spectrum (CD_3CN) of this complex in THF shows a single M-NO stretch at 1770 cm^{-1} , consistent with the presence of nonbridging, linear nitrosyl ligands. The ^1H NMR spectrum exhibits aromatic resonances and a single cyclopentadienyl resonance at δ 5.03 in a 1:1 ratio.⁷

The reaction of **1** with $\text{CpW}(\text{CO})_3\text{X}$ ($\text{X} = \text{Br}, \text{Cl}$) led ultimately to the formation of $[\text{CpW}(\text{CO})_3]_2$ and $[\text{CpCoNO}]_2$. Monitoring the reaction by IR and ^1H NMR spectroscopy showed the initial formation and subsequent decomposition of $[\text{Na}[\text{CpW}(\text{CO})_3]]$ during the reaction. Similar observations were made when **1** was treated with $\text{CpMo}(\text{CO})_3\text{X}$ ($\text{X} = \text{Cl}, \text{Br}$) or $\text{CpFe}(\text{CO})_3\text{X}$ ($\text{X} = \text{I}, \text{Br}$). No evidence was observed for the formation of any heteronuclear dimeric species in these reactions. However, when **1** was treated with an equimolar amount of $\text{CpCr}(\text{NO})_2\text{Cl}$, a new product was formed in about 50% yield as determined by the relative intensities of the cyclopentadienyl resonances in the ^1H NMR spectrum of the reaction mixture; the other major product of the reaction was $(\text{CpCoNO})_2$. Due to the instability of this complex toward column chromatography, the material was isolated as dark, air-stable crystals in only 11% yield from the crude reaction mixture by recrystallization from 1:3 hexane/ CH_2Cl_2 at -40°C . The new complex exhibits M-NO absorptions in THF at 1620 and 1520 (br) cm^{-1} and two Cp resonances of equal intensity in C_6D_6 at 4.6 and 4.2 ppm. On the basis of these data and a satisfactory elemental analysis, this complex is formulated as the heteronuclear bridging nitrosyl complex **5** (Scheme II). The M-NO stretch at 1620 cm^{-1} is assigned to the terminal NO ligand, and the broad absorbance at lower frequency is expected for bridging nitrosyls. This assignment is consistent with the stretching frequencies observed for the terminal and bridging nitrosyls occurring at 1670 and 1510 cm^{-1} (THF) in the structurally characterized $(\text{CpCr}(\text{NO})_2)_2$.⁸ Analogous products were not observed

(5) Calleri, M.; Ferraris, G.; Viterbo, D. *Acta Crystallogr.* **1966**, *20*, 93.

(6) Ferguson, G.; Fritchie, C. J.; Robertson, J. M.; Sin, G. A. *J. Chem. Soc.* **1961**, 1976.

(7) For other examples of metal nitrosyl-tin adducts, see: Cleland, A. J.; Fieldhouse, S. A.; Freeland, B. H.; Mann, C. D. M.; O'Brien, R. J. *J. Chem. Soc.* **1971**, 736. A previous Co-Sn complex is described by: Hackett, P.; Manning, A. R. *J. Organomet. Chem.* **1971**, *66*, C17.

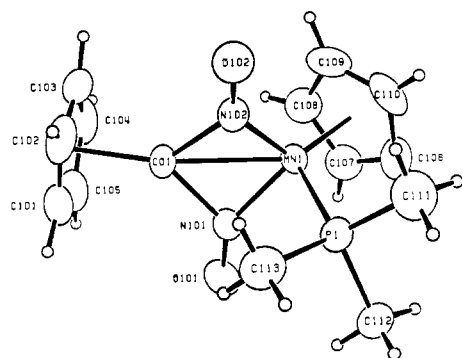


Figure 3. ORTEP drawing of complex 6.

Table I. Bond Lengths and Bond Angles of Complex 6^a

	molecule 1	molecule 2
Mn(1)–Co(1)	2.447 (1)	2.444 (1)
N(101)–Mn(1)	1.807 (1)	1.812 (2)
N(102)–Mn(1)	1.797 (1)	1.808 (2)
N(101)–Co(1)	1.804 (1)	1.796 (2)
N(102)–Co(1)	1.804 (1)	1.802 (2)
N(101)–O(101)	1.223 (2)	1.229 (2)
N(102)–O(102)	1.226 (2)	1.226 (2)
Mn(1)–Cp(12)	1.798 (1)	1.805 (1)
Co(1)–Cp(11)	1.759 (1)	1.744 (1)
P(1)–Mn(1)	2.267 (1)	2.270 (1)
Cp(11)–Co(1)–Mn(1)	165.42 (1)	164.74 (2)
Cp(12)–Mn(1)–Co(1)	134.83 (4)	133.67 (1)
Cp(12)–Mn(1)–P(1)	122.57 (2)	121.89 (2)
P(1)–Mn(1)–Co(1)	102.60 (2)	104.42 (2)
Co(1)–N(2)–Mn(1)	85.59 (7)	85.23 (7)
Co(1)–N(1)–Mn(1)	85.31 (7)	85.27 (7)

^a Corresponding values for the second molecule of the asymmetric unit are in brackets. Cp(12) is attached to Mn(1); Cp(11) is bound to Co(1).

in the reaction of 1 with $\text{CpM}(\text{NO})_2\text{Cl}$ ($\text{M} = \text{Mo}, \text{W}$).

In a similar manner, the reaction of 1 with $[\text{CpMn}(\text{CO})(\text{NO})(\text{PMe}_3)]\text{BF}_4$ (prepared by treatment of the known^{9a} complex $[\text{CpMn}(\text{CO})_2(\text{NO})]\text{BF}_4$ with PMe_3) in $\text{CH}_3\text{CN}/\text{THF}$ resulted in the formation of a new product in 75% yield, as determined by ^1H NMR analysis of the crude reaction mixture. Both $(\text{CpCoNO})_2$ and $(\text{CpMn}(\text{NO})(\text{PMe}_3))_2$ were observed as minor byproducts (<25%). The product was isolated as dark air-stable crystals in 30% yield after recrystallization from 3:2 toluene/hexane at -40°C . The pure complex exhibits a single M–NO stretch in THF at 1430 cm^{-1} and two ^1H NMR resonances of equal intensity in C_6D_6 at δ 4.5 (s) and 4.2 (d, $J_{\text{P-H}} = 3\text{ Hz}$). Analytical and spectroscopic data allow formulation of the species as the bridging nitrosyl dimer 6 (Scheme II). Similar stable products were observed in the reaction 1 with $[\text{CpMn}(\text{CO})_{3-x}(\text{NO})(\text{PPh}_3)_x]\text{BF}_4$ ($x = 0-2$) and $[\text{CpRe}(\text{CO})_2\text{NO}]\text{BF}_4$ but were formed in lower yield and could not be obtained in pure form. No product formation was observed in the reaction of 1 with $[\text{CpRe}(\text{CO})(\text{NO})(\text{PMe}_3)]\text{BF}_4$.

Complexes 5 and 6 represent, to our knowledge, the first examples of heterodinuclear complexes in which the two different metals are bridged only by NO groups.¹⁰ Therefore, the structure of complex 6 was determined by X-ray diffraction. Crystals of 5 suitable for X-ray diffraction analysis could not be obtained. The structure of 6 was solved and refined to a final R value of 2.23% and consists of two independent molecules in the triclinic unit cell. A Cp ring of one of the molecules is disordered; for the purposes of discussion, the ORTEP drawing of the fully ordered

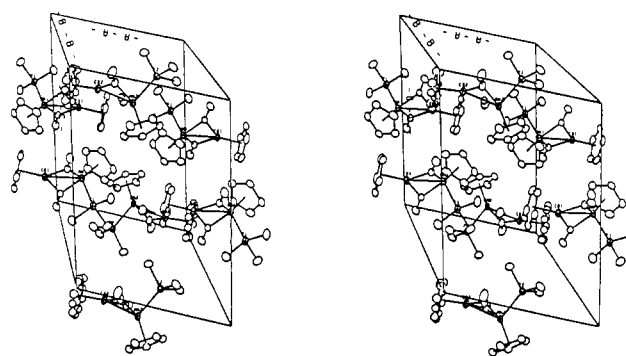


Figure 4. Stereoview of the unit cell of 6.

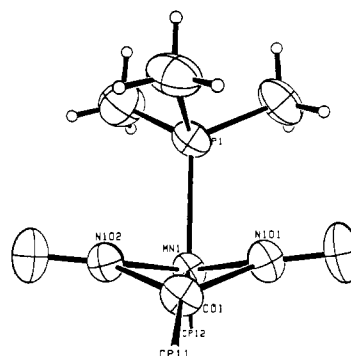
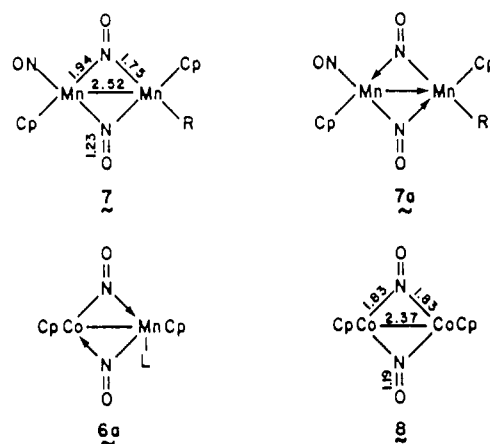


Figure 5. ORTEP drawing of 6 viewed down the Co(1)–Mn(1) axis. The Cp rings have been omitted for clarity.

Scheme III



molecule is shown in Figure 3, and the important bond distances and bond angles of both molecules are summarized in Table I. A stereoview of the unit cell is shown in Figure 4.

Perhaps the most important feature of this structure is the symmetrical placement of the bridging nitrosyl ligands with respect to the metal centers. It is interesting to compare this system with the manganese nitrosyl dimer 7, shown in Scheme III, which exhibits distinct asymmetry in the bridging nitrosyl ligands,¹¹ and with Tiripicchio's Cu–Ir complex,¹⁰ which has identical M–NO and M–N(pyridazine) bond lengths to both metals. One bonding arrangement for the manganese system that allows each metal center to attain an 18-electron configuration is represented by 7a. The bridging nitrosyls contribute three electrons to each metal center, requiring a Mn–Mn dative bond. Complex 6, however, needs a symmetrical single bond between metal centers (6a) to satisfy the EAN rule, while a bonding arrangement of the nitrosyl ligands is maintained similar to that in 7a. These results suggest

(8) Calderon, J. L.; Fontana, S.; Frauendorfer, E.; Day, V. W. *J. Organomet. Chem.* **1974**, *64*, C10.

(9) (a) Nesmeyanov, A. N.; Anisimov, K. N.; Kolbava, N. E.; Krasnolobodskaya, L. L. *Bull. Acad. Sci., USSR, Chem. Sci.* **1970**, *4*, 807. (b) Brunner, H. Z. *Anorg. Allg. Chem.* **1969**, *368*, 120.

(10) Recently a heterodinuclear complex containing a bridging NO and bis(pyridyl)pyridazine group was described: Tiripicchio, A.; Lanfredi, A. M. M.; Ghedini, M.; Neve, F. *J. Chem. Soc., Chem. Commun.* **1983**, 97.

(11) (a) Calderon, J. L.; Fontana, S.; Frauendorfer, E.; Day, V. W.; Stults, B. R. *Inorg. Chim. Acta* **1976**, *17*, L31. (b) Calderon, J. L.; Cotton, F. A.; DeBoer, B. G.; Martinez, N. *J. Chem. Soc., Chem. Commun.* **1971**, 1476.

the interesting principle that in the absence of a dative metal-metal bond, NO bridging will be highly symmetrical even in the presence of substantial differences in the nature and ligation of the two metal centers. The generality of this conclusion awaits the synthesis and structural characterization of additional members of the class of heteronuclear bridging nitrosyl dimers.

The Co-Mn distance of 2.45 Å is intermediate between the Co-Co distance of 2.37 Å in **8** and the Mn-Mn distance of 2.53 Å in **7**. One of the methyl groups of the phosphine ligand eclipses the Co-Mn bond and allows the nitrosyls to bend away from the Cp ring attached to the Mn atom, avoiding unfavorable steric interactions. The dihedral angle between the planes defined by N(2)-Mn-Co and Mn-Co-N(1) is 105.7° (Figure 5). The N-O bond distance of 1.23 Å lies between the values cited earlier for organic N-O single and double bonds.

Summary and Conclusion

The formulation of $(\text{CpCoNO})^-$ as a rare, low-valent transition-metal anion containing no additional back-bonding ligands to the metal center was confirmed by an X-ray diffraction analysis of its MeCp analogue, $\text{Na}(\text{CpCoNO})$ (**1**), which was previously shown to undergo clean reaction with alkyl halides to ultimately form the products of NO migratory insertion, was treated with a series of metal electrophiles. The reaction of **1** with ClSnR_3 ($\text{R} = \text{Me}, \text{Ph}$) and Ph_2SnCl_2 resulted in the clean conversion in moderate to good yield of the corresponding dinuclear and trinuclear Co-Sn adducts **2**, **3**, and **4**. The reaction of **1** with $\text{CpCr}(\text{NO})_2\text{Cl}$ and $[\text{CpMn}(\text{CO})(\text{NO})(\text{PMe}_3)]\text{BF}_4$ afforded heteronuclear bridging nitrosyl complexes **5** and **6**. These novel complexes were fully characterized and the structure of **6** was determined by X-ray diffraction. The results of this study showed the bridging nitrosyls to be symmetric with respect to the metal centers. The structure of **5** is based on the comparison of its M-NO stretching frequencies with those of the structurally characterized complex $(\text{CpCr}(\text{NO})_2)_2$.

Experimental Section

General Data. ^1H NMR spectra were recorded on a Varian EM-390 spectrometer at 250, 200, or 180 MHz on spectrometers equipped with Cryomagnets Inc. magnets, Nicolet model 1180 data collection systems, and multinuclear variable-temperature probes. All high-field instruments were constructed by Mr. Rudi Nulist in the UC Berkeley NMR laboratory. ^1H NMR spectra are recorded in units (parts per million downfield from tetramethylsilane). IR spectra were recorded on a Perkin-Elmer model 283 infrared spectrometer with 0.10-mm sodium chloride solution cells. All experiments were performed in a Vacuum Atmospheres Model 553-2 Dri-lab glovebox under a nitrogen atmosphere with attached M6-40-IH Dri-train and equipped with a -40 °C freezer.

Unless otherwise noted, reagents were obtained from commercial suppliers and used without further purification. The anions $\text{Na}[\text{CpCoNO}]$ and $\text{Na}[\text{MeCpCoNO}]$ as well as their corresponding PPN derivatives were prepared according to previously described procedures,² as were $\text{CpM}(\text{NO})_2\text{Cl}$ ($\text{M} = \text{Cr}, \text{Mo}, \text{W}$),¹⁴ $\text{CpM}(\text{CO})_3\text{X}$ ($\text{M} = \text{Mo}, \text{W}$; $\text{X} = \text{Cl}, \text{Br}$),¹⁵ $[\text{CpMn}(\text{CO})_2(\text{NO})(\text{PPh}_3)_x]\text{BF}_4$ ($x = 0, 1, 2$),⁹ $\text{CpFe}(\text{CO})_2\text{X}$ ($\text{X} = \text{Br}, \text{I}$),¹⁶ and $[\text{CpRe}(\text{CO})_3]\text{BF}_4$.^{9a} Tetrahydrofuran (THF), diethyl ether, benzene, and toluene were distilled from Na/benzophenone prior to use. Olefin free hexanes, purchased from Burdick and Jackson, were distilled under nitrogen from *n*-butyllithium. The acetonitrile and CH_2Cl_2 used were distilled under nitrogen from CaH_2 . Deuterated solvents were dried and deoxygenated using the methods described above.

Elemental analyses were performed by the Microanalytical Laboratory operated by the College of Chemistry, UCB. Melting points were carried out in sealed capillaries under nitrogen on a Thomas-Hoover capillary

melting point apparatus and are uncorrected.

CpCoNO(Sn(CH₃)₃)₂ (2**).** A 10-mL THF solution containing 450 mg (2.26 mmol) of ClSnMe_3 (Alfa) was added to a stirred 25-mL THF solution containing 400 mg (2.26 mmol) of **1**. The reaction mixture immediately became dark red in color. After the solution was allowed to stir for an additional 30 min, the solvent was removed by vacuum transfer. The red oil remaining was redissolved in benzene and filtered through a fine glass frit. The solvent was again removed by vacuum transfer to yield 474 mg (1.49 mmol, 66%) of a viscous, air-sensitive red oil, which was analytically pure: IR (THF) 1760 (s) cm^{-1} ; ^1H NMR (C_6D_6) δ 4.50 (s, 5 H), 0.55 (t, 9 H, $J_{\text{Sn-H}} = 25$ Hz, 20% intensity). Anal. Calcd for $\text{C}_8\text{H}_{14}\text{NOCOSn}$: C, 30.23; H, 4.45; N, 4.41. Found: C, 30.51; H, 4.45; N, 4.44.

CpCoNO(Sn(C₆H₅)₂)₂ (3**).** A 5-mL THF solution containing 326 mg (0.874 mmol) of ClSnPh_3 (Alfa) was added to a stirred solution of 200 mg (1.13 mmol) of **1** in 20 mL of THF. Upon addition, the reaction solution became brownish. The solvent was removed by vacuum transfer, and the remaining brown solid was dissolved in benzene and filtered as described above. The crude solid obtained after solvent removal was recrystallized at -40 °C from a 3:1 pentane/toluene solution to yield 155 mg (0.308 mmol, 36% based on Sn) of **3** as dark red, air-stable needles: mp 106 °C; IR (THF) 1770 (s) cm^{-1} ; ^1H NMR (CD_3CN) δ 7.5 (m, 18 H, $J_{\text{Sn-H}} = 25$ Hz, 20% intensity), 5.06 (s, 5 H). Anal. Calcd for $\text{C}_{23}\text{H}_{20}\text{NOCOSn}$: C, 54.80; H, 4.01; N, 2.78. Found: C, 54.52; H, 3.99; N, 3.01.

(CpCoNO)₂Sn(C₆H₅)₂ (4**).** A 5-mL THF solution containing 194 mg (0.565 mmol) of Cl_2SnPh_2 (Alfa) was added with stirring to a 25-mL THF solution of 250 mg (1.41 mmol) of **1**. The reaction mixture became red-brown and was allowed to stir for 15 min. The solvent was removed by vacuum transfer, and the residue was filtered as described above. The final crude solid was recrystallized from hexane at -40 °C to yield 210 mg (0.362 mmol, 64% based on Sn) of **4** as deep red air-sensitive needles, which became a waxy solid at room temperature: IR (THF) 1760 (s) cm^{-1} ; ^1H NMR (CD_3CN) δ 7.6 (m, 10 H, $J_{\text{Sn-H}} = 25$ Hz, 20% intensity), 5.03 (s, 10 H). Anal. Calcd for $\text{C}_{22}\text{H}_{20}\text{N}_2\text{O}_2\text{Co}_2\text{Sn}$: C, 45.48; H, 3.48; N, 4.82. Found: C, 45.68; H, 3.61; N, 4.78.

[CpM(CO)(NO)P(CH₃)₃]₂BF₄ ($\text{M} = \text{Mn}, \text{Re}$). A 30-mL CH_3CN solution containing 1.0 g (3.41 mmol) of $[\text{CpMn}(\text{CO})_2\text{NO}]\text{BF}_4$ was degassed on a Schlenk line. The reaction flask was cooled in liquid N_2 , and 259 mg (3.41 mmol) of PMe_3 (Alfa) was vacuum transferred into the reaction vessel. Before being thawed, the reaction mixture was placed under a positive nitrogen flow. As the reaction mixture warmed to room temperature, intense bubbling was observed. The solution was allowed to stir for 3 h, and the solvent was removed by vacuum transfer. The solid residue remaining was recrystallized from 1:5 $\text{Et}_2\text{O}/\text{CH}_3\text{CN}$ at -40 °C to yield 0.580 g (2.53 mmol, 67%) of $[\text{CpMn}(\text{CO})(\text{NO})(\text{PMe}_3)]\text{BF}_4$: IR (CH_3CN) 2030 (s), 1800 (s) cm^{-1} ; ^1H NMR (CD_3CN) δ 5.51 (d, $J_{\text{P-H}} = 1.9$ Hz, 5 H), 1.70 (d, $J_{\text{P-H}} = 11.6$ Hz, 9 H). Anal. Calcd for $\text{C}_9\text{H}_{14}\text{MnNO}_2\text{PBF}_4$: C, 31.72; H, 4.15; N, 4.11. Found: C, 32.03; H, 4.28; N, 4.02.

Following the identical procedure described above, 500 mg (1.49 mmol) of $[\text{CpRe}(\text{CO})(\text{NO})\text{NCCH}_3]\text{BF}_4$ ¹⁷ in 20 mL of CH_3CN was treated with 114 mg (1.49 mmol) of PMe_3 to yield 342 mg (0.894 mmol, 60%) of $[\text{CpRe}(\text{CO})(\text{NO})(\text{PMe}_3)]\text{BF}_4$: IR (CH_3CN) 2010 (s), 1750 (s) cm^{-1} ; ^1H NMR (CD_3CN) δ 5.60 (d, $J_{\text{P-H}} = 0.8$ Hz, 5 H), 1.90 (d, $J_{\text{P-H}} = 11.7$ Hz, 9 H). Anal. Calcd for $\text{C}_9\text{H}_{14}\text{ReNO}_2\text{PBF}_4$: C, 22.87; H, 2.99; N, 2.97. Found: C, 23.29; H, 3.17; N, 3.03.

Reaction of **1 with $\text{CpM}(\text{CO})_3\text{X}$ ($\text{M} = \text{Mo}, \text{W}$, $\text{X} = \text{Cl}, \text{Br}$, $n = 0$; $\text{M} = \text{Fe}$, $\text{X} = \text{Br}$, $n = 1$).** In a typical reaction, 20 mg (0.113 mmol) of **1** in 1 mL of THF was reacted with an equimolar amount of the substrate in CH_3CN . The reaction was monitored by IR spectroscopy and revealed the formation of the corresponding metal carbonyl anion. The reaction solutions subsequently decomposed to the metal carbonyl dimer and $(\text{CpCoNO})_2$. After solvent removal by vacuum transfer, these species were observed as the only C_6D_6 soluble products in the ^1H NMR analysis of the reaction crude. The identities of all species were determined by spectroscopic comparison with authentic samples.

Cp₂CoCr(NO)₃ (5**).** A solution of 637 mg (3.0 mmol) of $\text{CpCr}(\text{NO})_2\text{Cl}$ in 10 mL of THF was added to a stirred solution of 530 mg (3.0 mmol) of **1** in 25 mL of THF. The resulting mixture was allowed to stir for an additional 30 min. The solvent was removed by vacuum transfer leaving a dark green solid from which $(\text{CpCoNO})_2$ was extracted by stirring over ten 20-mL portions of hexanes or until the hexane extracts were colorless. The resulting olive green solid was then dissolved in benzene and filtered through a fine glass frit. The solid obtained after

(12) Bernal, I.; Korp, J. D.; Reisner, G. M.; Hermann, W. A. *J. Organomet. Chem.* **1977**, *139*, 321.

(13) Huheey, J. E. "Inorganic Chemistry", 2nd ed.; Harper and Row: New York, 1978; p 232.

(14) Hoyano, J. K.; Legzdins, P.; Malito, J. Y. *Inorg. Synth.* **1978**, *18*, 126.

(15) (a) Piper, T. S.; Wilkinson, G. J. *Inorg. Nucl. Chem.* **1956**, *3*, 104. (b) Alway, D. G.; Barnett, K. W. *Inorg. Chem.* **1980**, *19*, 1533.

(16) King, R. B. "Organometallic Synthesis", Academic Press: New York, 1965; Vol. 1, p 175.

(17) Tam, W.; Lin, G.; Wong, W.; Kiel, W. A.; Wong, V. K.; Gladysz, J. A. *J. Am. Chem. Soc.* **1982**, *104*, 141.

(18) For examples of other compounds in which tin-aryl hydrogen coupling constants have been measured, see: (a) Verdonck, L.; van der Kelen, G. P. *Bull. Soc. Chim. Belg.* **1965**, *74*, 361. (b) Randall, E. W.; Zuckerman, J. J. *J. Am. Chem. Soc.* **1968**, *90*, 3167.

solvent removal was recrystallized from 1:3 hexane/ CH_2Cl_2 at -40°C to yield 105 mg (0.317 mmol, 11%) of **5** as dark air-stable crystals which did not melt below 290°C . IR (THF) 1680 (m), 1520 (w, br) cm^{-1} ; ^1H NMR (C_6D_6) δ 4.80 (s, 5 H), 4.47 (s, 5 H). Anal. Calcd for $\text{C}_{10}\text{H}_{10}\text{N}_3\text{O}_3\text{CoCr}$: C, 36.27; H, 3.07; N, 12.69. Found: C, 35.98; H, 3.01; N, 12.47.

Reaction of 1 with $\text{CpM}(\text{NO})\text{Cl}$ ($\text{M} = \text{Mo}, \text{W}$). According to the procedure described above, 20-mg (0.113-mmol) quantities of **1** were reacted with equimolar amounts of $\text{CpM}(\text{NO})_2\text{Cl}$ ($\text{M} = \text{Mo}, \text{W}$) in THF. The reactions were monitored by IR spectroscopy, which revealed only the presence of $(\text{CpCoNO})_2$ (IR (THF) 1590 (w), 1540 (s) cm^{-1}) as the major reaction product. ^1H NMR analysis in C_6D_6 of the crude product showed small amounts of decomposition products and mostly $(\text{CpCoNO})_2$ (^1H NMR (C_6D_6) δ 4.53 (s)).

$\text{Cp}_2\text{CoMn}(\text{NO})_2\text{P}(\text{CH}_3)_3$ (6**).** A 5-mL CH_3CN solution of 961 mg (2.82 mmol) of $[\text{CpMn}(\text{CO})(\text{NO})\text{PMe}_3]\text{BF}_4$ was added to a stirred solution of 500 mg (2.82 mmol) of **1** in 25 mL of THF. The reaction solution turned a dark blue-black and was allowed to stir for 15 min. After the solvent was removed by vacuum transfer, the solid remaining was dissolved in benzene and filtered through a fine frit. The dark solid remaining after solvent removal was recrystallized from 3:2 hexane/toluene at -40°C to afford 325 mg (0.855 mg, 30%) of dark air-stable crystals: mp 119°C ; IR (THF) 1460 (s) cm^{-1} ; ^1H NMR (C_6D_6) δ 4.88 (s, 5 H), 4.38 (d, $J_{\text{P-H}} = 1.4$ Hz, 5 H), 0.34 (d, 9 H, $J_{\text{P-H}} = 9.5$ Hz). Anal. Calcd for $\text{C}_{13}\text{H}_{19}\text{N}_2\text{O}_2\text{PCoMn}$: C, 41.07; H, 5.04; N, 7.37. Found: C, 41.10; H, 5.12; N, 7.22.

Reaction of 1 with $[\text{CpMn}(\text{CO})_{3-x}(\text{NO})(\text{PPh}_3)_x]\text{BF}_4$ ($x = 0-2$) and $[\text{CpRe}(\text{CO})_{3-x}(\text{NO})(\text{PMe}_3)_x]\text{BF}_4$ ($x = 0, 1$). A 1-mL CH_3CN solution of 33 mg (0.113 mmol) of $[\text{CpMn}(\text{CO})_2(\text{NO})]\text{BF}_4$ was added to 20 mg (0.113 mmol) of **1** in 2 mL of THF. The solvent was removed by vacuum transfer after the reaction was allowed to stir for 15 min. ^1H NMR spectroscopic analysis of the crude reaction products soluble in C_6D_6 showed a new product displaying two Cp singlets of equal intensity at δ 4.66 and 4.50 was formed in 50% yield, based on integration against the Cp resonances of $(\text{CpCoNO})_2$, the only other observable species. The new product is presumably the derivative of **6**, where a CO ligand replaces the PMe_3 group bound to the Mn atom. With use of the same procedure, the reaction of **1** with $[\text{CpMn}(\text{CO})(\text{NO})\text{PPh}_3]\text{BF}_4$ and $[\text{CpMn}(\text{NO})(\text{PPh}_3)_2]\text{BF}_4$ resulted in the formation of a new product in 75% and 65% yields, respectively. The ^1H NMR (C_6D_6) spectrum of this product (contaminated with $(\text{CpCoNO})_2$) displays two Cp singlets of equal intensity at δ 4.59 and 4.48, in addition to the resonances associated with bound PPh_3 . This product is presumably the analogue of **6** having a PPh_3 ligand bound to the Mn center. Although these products were apparently formed in reasonable yield, none could be isolated in pure form. The products were unstable to chromatographic conditions (SiO_2 , Al_2O_3) and could not be purified by recrystallization.

According to the above procedures, **1** was treated with an equivalent amount of $[\text{CpRe}(\text{CO})(\text{NO})(\text{PMe}_3)]\text{BF}_4$. ^1H NMR analysis of the crude reaction product in C_6D_6 showed only the presence of $(\text{CpCoNO})_2$. In the reaction of **1** with $[\text{CpRe}(\text{CO})_2(\text{NO})]\text{BF}_4$, ^1H NMR analysis of the initial reaction mixture revealed a new product that displayed two Cp singlets of equal intensity at δ 4.76 and 4.64, formed in 20% yield based on the integration against the Cp resonance of the only other observable product $(\text{CpCoNO})_2$. Isolation of this material was not attempted.

Crystal Structure Determination of 1a. Large orange-red crystals of **1a** were obtained by slow recrystallization from 4:1 $\text{Et}_2\text{O}/\text{CH}_3\text{CN}$. Fragments cleaved from these crystals were mounted in glass capillaries in air; the capillaries were flushed in dry nitrogen and then flame sealed. Preliminary precession photographs showed no symmetry higher than an inversion center.

The first of the two crystals used was then transferred to an Enraf-Nonius CAD-4 diffractometer¹⁹ and centered in the beam. Automatic peak search and indexing procedures gave a triclinic reduced primitive unit cell, and inspection of the Niggli values revealed no conventional cells of symmetry higher than triclinic. The final cell parameters and pertinent details of the data collection procedure are given in Table II. The first crystal decomposed in the X-ray beam to the point where it was no longer usable, so a second crystal was mounted and used to continue the data set with a suitable overlap in the data. The 1141 reflections collected on the first crystal just before the loss of the same were rejected from the data set during processing.

(19) For details on the instrumentation, data reduction formulae, and other related information, see: Theopold, K. H.; Bergman, R. G. *Organometallics* **1982**, *1*, 1571 (ref 19-26).

(20) Reflections used for azimuthal scans were located near $\chi = 90^\circ$, and the intensities were measured at 10° increments of rotation of the crystal about the diffraction vector.

Table II. Crystal and Data Collection Parameters

	$\text{C}_{14}\text{H}_{40}\text{N}_3\text{O}_2\text{P}_2\text{Co}$ (1a)	$\text{C}_{13}\text{H}_{19}\text{N}_2\text{O}_2\text{CoMnP}$ (6)
(A) Crystal Parameters at 25°C^a		
<i>a</i> , Å	8.7954 (22)	9.7411 (7)
<i>b</i> , Å	15.4459 (24)	13.0004 (8)
<i>c</i> , Å	15.7608 (21)	13.6768 (14)
α , deg	77.730 (12)	77.554 (7)
β , deg	75.114 (15)	77.960 (7)
γ , deg	72.685 (15)	68.942 (6)
<i>V</i> , Å ³	1953.9 (7)	1561.9 (2)
space group	$P\bar{1}$	$P\bar{1}$
<i>M_r</i>	747.7	380.15
<i>Z</i>	2	4
<i>d</i> (calcd), g cm ⁻³	1.271	1.62
μ (calcd), cm ⁻¹	5.53	19.39
size, mm	see text	$0.16 \times 0.21 \times 0.36$
(B) Data Measurement Parameters		
diffractometer	Enraf-Nonius CAD-4	
radiation	Mo K α ($\lambda = 0.71073$ Å)	
monochromator	highly oriented graphite ($2\theta_m = 12.2^\circ$); perpendicular mode, assumed 50% perfect	
detector	crystal scintillation counter, with pulse-height analyzer	
aperture-crystal	173	
dist, mm		
vertical sperture, mm	3.0	
horizontal aperture, mm	$(2 + 1.0 \tan \theta)$ (variable)	
reflectns measd	$+h, \pm k, \pm l$	
2θ range, deg	3-45	
scan type	$\theta-2\theta$	
scan speed (θ), deg/min	0.6-6.7	
scan width ($\Delta\theta$)	$(0.5 + 0.347 \tan \theta)$	
bkgd	0.25 ($\Delta\theta$) at each end of scan	
reflectns collected	6385	4067
unique reflectns	5090	4067
std reflectns	(0,4,10), (0,10,1), (255), (268), (410) (5,0,1)	
orientatn	measured every 2 h of X-ray exposure time; over the period of data collection significant decay in intensity was observed for 1a ; crystal I, 20%; crystal II, 5%; no decay of intensity was observed for 6 . three reflections were checked every 250 measurements; crystal orientation was redetermined if any of the reflections were offset from their predicted positions by more than 0.1%; reorientation of 1a was needed several times during data collection; reorientation of 6 was not necessary.	

^a Unit cell parameters and their esd's were derived by a least-squares fit to the setting angles of the unresolved Mo K α components of 24 reflections with 2θ between 24 and 29° for **1a** and near 28° for **6**.

The 6231 raw intensity data were converted to structure factor amplitudes and their esds by correction for scan speed, background, and Lorentz and polarization effects.¹⁸ Inspection of the azimuthal scan data¹⁹ for the second crystal showed a variation of $I_{\text{min}}/I_{\text{max}} = 0.92$ for the average curve. No absorption correction was applied to the data since they were not all from this crystal. Each of the two crystals used decomposed with time in the X-ray beam as shown by the standard reflections. The "decay curve" was used to correct for this decomposition and to scale together the data from the two different crystals. Removal of the redundant data taken on the first crystal left 5090 unique data.

The structure was solved by Patterson methods and refined via standard least-squares and Fourier techniques. The assumption that the space group was the centric $P\bar{1}$ was confirmed by successful refinement.

A difference Fourier map calculated after all non-hydrogen atoms had been refined with anisotropic thermal parameters revealed peaks in locations expected for all hydrogen atoms save those of the acetonitrile. Hydrogen atom positions were then calculated on the basis of idealized geometry at the carbon atoms and $d(\text{C-H}) = 0.95$ Å. The hydrogen

Table III. Positional and Equivalent Thermal Parameters for Non-Hydrogen Atoms in **1a**^a

atom	x	y	z	B, Å ²
Co	0.17676 (4)	0.25414 (2)	0.20941 (2)	3.658 (9)
P(1)	0.69730 (8)	0.23475 (4)	0.58741 (4)	2.88 (1)
P(2)	0.47653 (8)	0.22825 (4)	0.76590 (4)	2.94 (1)
O	0.0800 (2)	0.3198 (1)	0.3738 (1)	4.96 (5)
N(1)	0.1246 (2)	0.2883 (1)	0.3035 (1)	3.58 (5)
N(2)	0.5486 (2)	0.2192 (1)	0.6648 (1)	3.62 (5)
N(3)	0.6660 (6)	0.4356 (4)	0.0731 (3)	15.9 (2)
C(1)	0.1048 (4)	0.2751 (2)	0.0889 (2)	4.99 (8)
C(2)	0.2537 (4)	0.2981 (2)	0.0753 (2)	5.80 (9)
C(3)	0.3681 (4)	0.2192 (2)	0.1030 (2)	5.70 (9)
C(4)	0.2894 (4)	0.1474 (2)	0.1339 (2)	5.10 (8)
C(5)	0.1266 (3)	0.1822 (2)	0.1252 (2)	4.35 (7)
C(6)	0.0052 (4)	0.1288 (2)	0.1428 (2)	6.01 (9)
C(7)	0.5444 (6)	0.4441 (3)	0.1241 (3)	10.2 (1)
C(8)	0.3959 (6)	0.4530 (3)	0.1882 (3)	9.6 (2)
C(11)	0.8727 (3)	0.1378 (2)	0.5901 (2)	3.13 (6)
C(12)	1.0293 (3)	0.1467 (2)	0.5511 (2)	4.07 (7)
C(13)	1.1587 (4)	0.0706 (2)	0.5525 (2)	5.03 (8)
C(14)	1.1347 (4)	-0.0145 (2)	0.5909 (2)	5.16 (8)
C(15)	0.9813 (4)	-0.0243 (2)	0.6270 (2)	4.70 (8)
C(16)	0.8501 (3)	0.0518 (2)	0.6273 (2)	3.88 (7)
C(17)	0.6359 (3)	0.2441 (2)	0.4848 (2)	3.00 (6)
C(18)	0.7425 (3)	0.2609 (2)	0.4048 (2)	3.79 (7)
C(19)	0.7002 (4)	0.2614 (2)	0.3258 (2)	4.74 (8)
C(20)	0.5563 (4)	0.2440 (2)	0.3265 (2)	5.47 (8)
C(21)	0.4512 (3)	0.2278 (2)	0.4048 (2)	5.76 (8)
C(22)	0.4893 (3)	0.2282 (2)	0.4851 (2)	4.31 (7)
C(23)	0.7608 (3)	0.3355 (2)	0.5864 (2)	3.37 (6)
C(24)	0.7012 (4)	0.4175 (2)	0.5351 (2)	4.60 (8)
C(25)	0.7431 (4)	0.4961 (2)	0.5410 (2)	6.3 (1)
C(26)	0.8411 (4)	0.4929 (2)	0.5965 (2)	6.90 (9)
C(27)	0.8999 (4)	0.4116 (2)	0.6480 (2)	6.20 (8)
C(28)	0.8604 (3)	0.3321 (2)	0.6431 (2)	4.64 (7)
C(29)	0.3955 (3)	0.1313 (2)	0.8174 (2)	3.07 (6)
C(30)	0.3628 (3)	0.0799 (2)	0.7649 (2)	4.21 (7)
C(31)	0.3062 (4)	0.0031 (2)	0.8043 (2)	4.94 (8)
C(32)	0.2821 (3)	-0.0219 (2)	0.8947 (2)	4.62 (8)
C(33)	0.3127 (3)	0.0290 (2)	0.9466 (2)	4.27 (7)
C(34)	0.3700 (3)	0.1053 (2)	0.9088 (2)	3.67 (7)
C(35)	0.3179 (3)	0.3324 (2)	0.7789 (2)	3.19 (6)
C(36)	0.3193 (4)	0.4077 (2)	0.7131 (2)	4.82 (8)
C(37)	0.2039 (4)	0.4899 (2)	0.7246 (2)	5.60 (9)
C(38)	0.0869 (4)	0.4974 (2)	0.8005 (2)	4.91 (8)
C(39)	0.0840 (4)	0.4236 (2)	0.8652 (2)	5.23 (9)
C(40)	0.1977 (4)	0.3407 (2)	0.8550 (2)	4.47 (8)
C(41)	0.6234 (3)	0.2264 (2)	0.8281 (2)	3.20 (6)
C(42)	0.6088 (3)	0.2977 (2)	0.8721 (2)	4.62 (7)
C(43)	0.7288 (4)	0.2935 (2)	0.9165 (2)	6.19 (9)
C(44)	0.8612 (4)	0.2195 (2)	0.9164 (2)	6.11 (9)
C(45)	0.8765 (4)	0.1482 (2)	0.8736 (2)	5.63 (9)
C(46)	0.7570 (4)	0.1507 (2)	0.8301 (2)	4.48 (8)

^a Atoms refined with isotropic thermal parameters. Anisotropically refined atoms are given in the form of the isotropic equivalent thermal parameter defined as $(4/3)[a^2B(1,1) + b^2B(2,2) + c^2B(3,3) + ab(\cos \gamma)B(1,2) + ac(\cos \beta)B(1,3) + bc(\cos \alpha)B(2,3)]$.

atoms were included in the structure factor calculations but were not refined. In the final cycles of least squares a secondary extinction parameter was refined.²¹ The final residuals for 461 variables refined against the 3998 data for which $F^2 > 3\sigma(F^2)$ were $R = 3.09\%$, $wR = 4.50\%$, and $GOF = 1.729$. The R value for all 5090 data was 5.23%.

The quantity minimized by the least-squares program was $\sum w(|F_o| - |F_c|)^2$, where w is the weight of a given observation. The p factor, used to reduce the weight of the intense reflections, was set to 0.04 throughout the refinement. The largest peaks in the final difference Fourier map had electron densities of ca. 0.2 e/Å³ and were located near the acetonitrile molecule. The positional and equivalent thermal parameters of non-hydrogen atoms are given in Table III. Anisotropic thermal parameter, the positions of the hydrogen atoms, and a listing of the values of F_o and F_c are available as supplementary material.

Crystal Structure Determination of 6. Well-formed, moderate sized black crystals of **6** were obtained by slow crystallization from 4:1 CH₂Cl₂/hexane at -40 °C. Selected crystals were mounted in capillaries

Table IV. Positional and Equivalent Thermal Parameters for Non-Hydrogen Atoms in **6**

atom	x	y	z	B, Å ²
Co(1)	0.16358 (3)	0.23636 (3)	0.39614 (3)	2.809 (7)
Co(2)	0.22391 (3)	-0.25509 (3)	0.14084 (3)	3.400 (8)
Mn(1)	-0.10561 (3)	0.32043 (3)	0.39915 (3)	2.461 (8)
Mn(2)	0.44643 (3)	-0.22316 (3)	0.16455 (3)	2.583 (8)
P(1)	-0.16000 (6)	0.20316 (5)	0.32410 (5)	3.09 (1)
P(2)	0.62243 (7)	-0.29640 (5)	0.03770 (5)	3.02 (1)
O(101)	-0.0030 (2)	0.1303 (2)	0.5475 (2)	4.63 (5)
O(102)	0.0753 (2)	0.3661 (2)	0.2144 (1)	4.40 (5)
O(201)	0.4328 (2)	-0.4455 (1)	0.2251 (2)	4.54 (5)
O(202)	0.2872 (2)	-0.0778 (2)	0.0066 (2)	6.27 (6)
N(101)	0.0089 (2)	0.1979 (2)	0.4716 (2)	2.99 (5)
N(102)	0.0489 (2)	0.3186 (2)	0.3004 (2)	2.88 (5)
N(201)	0.3938 (2)	-0.3473 (2)	0.1853 (2)	3.05 (5)
N(202)	0.3190 (2)	-0.1593 (2)	0.0726 (2)	3.82 (5)
C(101)	0.3700 (3)	0.1101 (2)	0.4080 (2)	3.99 (7)
C(102)	0.3828 (3)	0.1882 (3)	0.3240 (2)	4.38 (7)
C(103)	0.3514 (3)	0.2907 (2)	0.3564 (3)	4.91 (8)
C(104)	0.3209 (3)	0.2737 (2)	0.4617 (2)	4.65 (7)
C(105)	0.3295 (3)	0.1627 (2)	0.4932 (2)	4.10 (7)
C(106)	-0.3389 (3)	0.4014 (2)	0.4494 (2)	4.26 (7)
C(107)	-0.2600 (3)	0.3906 (2)	0.5274 (2)	3.81 (7)
C(108)	-0.1595 (3)	0.4489 (2)	0.4902 (2)	4.03 (7)
C(109)	-0.1781 (3)	0.4978 (2)	0.3898 (2)	4.49 (8)
C(110)	-0.2888 (3)	0.4686 (2)	0.3641 (2)	4.45 (8)
C(111)	-0.2636 (3)	0.2689 (3)	0.2184 (2)	5.32 (8)
C(112)	-0.2652 (3)	0.1202 (2)	0.4070 (3)	4.53 (7)
C(113)	0.0014 (3)	0.0986 (2)	0.2705 (3)	4.93 (8)
C(201)	0.0156 (6)	-0.2467 (4)	0.2438 (4)	3.9 (1) ^a
C(202)	0.0834 (6)	-0.3517 (4)	0.2076 (4)	3.7 (1) ^a
C(203)	0.0969 (6)	-0.3325 (5)	0.0943 (4)	4.1 (1) ^a
C(204)	0.0389 (5)	-0.2124 (4)	0.0632 (4)	3.5 (1) ^a
C(205)	-0.0111 (5)	-0.1584 (4)	0.1521 (4)	3.4 (1) ^a
C(201)'	0.0471 (6)	-0.3019 (5)	0.2395 (4)	4.1 (1) ^a
C(202)'	0.0882 (6)	-0.3531 (4)	0.1548 (4)	3.8 (1) ^a
C(203)'	0.0580 (6)	-0.2720 (5)	0.0767 (5)	4.5 (1) ^a
C(202)''	0.0024 (6)	-0.1739 (5)	0.1104 (5)	4.8 (1) ^a
C(205)'	-0.0079 (6)	-0.1913 (4)	0.2105 (4)	4.0 (1) ^a
C(206)	0.6131 (3)	-0.2096 (2)	0.2391 (2)	4.10 (7)
C(207)	0.5432 (3)	-0.1048 (2)	0.1848 (2)	4.11 (6)
C(208)	0.3926 (3)	-0.0712 (2)	0.2256 (2)	4.12 (7)
C(209)	0.3690 (3)	-0.1554 (2)	0.3046 (2)	3.69 (6)
C(210)	0.5067 (3)	-0.2402 (2)	0.3137 (2)	3.70 (6)
C(211)	0.7028 (3)	-0.1976 (3)	-0.0443 (2)	5.20 (8)
C(212)	0.7824 (4)	-0.4136 (3)	0.0719 (3)	5.45 (9)
C(213)	0.5563 (3)	-0.3501 (3)	-0.0477 (2)	5.83 (8)
Cp(11)	0.3509	0.2051	0.4084	<i>b</i>
Cp(12)	-0.2451	0.4415	0.4442	<i>b</i>
Cp(21)	0.0448	-0.2603	0.1522	<i>b</i>
Cp(22)	0.4849	-0.1562	0.2535	<i>b</i>

^a Atoms refined with isotropic thermal parameters and $G = 0.50$.

^b Geometric centroids of the cyclopentadiene rings. Anisotropically refined atoms are given in the form of the isotropic equivalent thermal parameter defined as $(4/3)[a^2B(1,1) + b^2B(2,2) + c^2B(3,3) + ab(\cos \gamma)B(1,2) + ac(\cos \beta)B(1,3) + bc(\cos \alpha)B(2,3)]$.

as for **1a**. Preliminary precession photographs indicated triclinic Laue symmetry.

The crystal used for data collection was then transferred to the diffractometer and centered in the beam. Automatic peak search and indexing procedures yielded a triclinic reduced primitive cell, with a volume consistent with $Z = 4$. Inspection of the Niggli values revealed no conventional cells of higher symmetry, however, and the space group was assumed to be $P\bar{1}$ with two molecules in the asymmetric unit. The final cell parameters and specific data collection parameters are given in Table II.

The 4067 raw intensity data were converted to structure factor amplitudes and their esds as above. No correction for crystal decomposition was necessary. Inspection of the azimuthal scan²⁰ data showed a variation $I_{\min}/I_{\max} = 0.80$ for the average curve. An absorption correction based on the measured shape and size of the crystal and a $10 \times 10 \times 8$ Gaussian grid of internal points was applied to the data after solution and isotropic refinement of the structure ($T_{\max} = 0.794$, $T_{\min} = 0.630$).

The structure was solved by Patterson methods and refined via standard least-squares and Fourier techniques. The identity of the metal atoms was determined by their coordination. The assumption that the space group was $P\bar{1}$ was confirmed by the successful solution and re-

finement of the structure. The initial assignment of disorder for one Cp ring started at 70%–30% but refined toward 50%–50%, where it was fixed for the remainder of the refinement. Except for the hydrogens on the disordered Cp ring, hydrogens were included in the structure factor calculations as for **1a**.

Inspection of the residuals showed that the data was affected by secondary extinction, and an extinction parameter²¹ was refined in subsequent cycles of least squares. Inspection of the penultimate difference Fourier map showed a ring of electron density around the periphery of the disordered Cp ring. Half-occupancy hydrogen atom positions were then calculated and included in the structure factor calculations.

The final residuals for 356 variables refined against the 3537 data for which $F^2 > 3\sigma(F^2)$ were $R = 2.23\%$, $wR = 3.11\%$, and $GOF = 2.071$ (the corresponding values for the model without the half-occupancy hydrogens were $R = 2.55\%$, $wR = 4.07\%$, $GOF = 2.704$). The R value for all 4067 data was 2.96%.

The p factor for the weighting scheme was set to 0.02 during the last cycles of least-squares refinement. The largest peaks in the final difference Fourier map had electron densities of 0.20–0.36 e/Å³ and were located near the disordered Cp ring. The positional and equivalent thermal parameters of nonhydrogen atoms are given in Table IV; anisotropic thermal parameters, positions of the hydrogen atoms, and the

values of F_o and F_c are available as supplementary material.

Acknowledgment. We appreciate financial support of this work from National Institutes of Health Grant No. GM-25459. R.G.B. is also grateful for a Sherman Fairchild Distinguished Scholarship from the California Institute of Technology (1984).

Registry No. **1**, 78305-62-1; Na⁺**1a**, 85454-65-5; PPN⁺**1a**·CH₃CN, 92284-05-4; **2**, 92269-84-6; **3**, 92269-85-7; **4**, 92269-86-8; **5**, 92269-87-9; **6**, 92269-88-0; Cp₂CoMn(NO)₂CO, 92269-91-5; Cp₂CoMn(NO)₂PPh₃, 92269-92-6; [CpMn(CO)(NO)(PMe₃)]BF₄, 92269-90-4; [CpRe(CO)(NO)(PMe₃)]BF₄, 89727-22-0; (CpCoNO)₂, 51862-20-5; [CpMn(CO)₂NO]BF₄, 31960-39-1; [CpRe(CO)(NO)NCCH₃]BF₄, 92269-93-7; CpCr(NO)₂Cl, 12071-51-1; CpMo(NO)₂Cl, 12305-00-9; CpW(NO)₂Cl, 53419-14-0; [CpRe(CO)₂(NO)]BF₄, 31960-40-4; (MeCpCoNO)₂, 85454-64-4; ClSnMe₃, 1066-45-1; ClSnPh₃, 639-58-7; Cl₂SnPh₂, 1135-99-5.

Supplementary Material Available: A listing of observed and calculated structure factors for complexes PPN⁺**1a** and **6** (57 pages). Ordering information is given on any current masthead page.

Efficient Host-to-Guest Excited-State Energy Transfer in a Lamellar Solid: Photoluminescence and Photoaquation of Hexaamminechromium(III)-Substituted Hydrogen Uranyl Phosphate

Michael M. Olken and Arthur B. Ellis*

Contribution from the Department of Chemistry, University of Wisconsin—Madison, Madison, Wisconsin 53706. Received June 11, 1984

Abstract: A layered solid of approximate composition H_{0.7}[Cr(NH₃)₆]_{0.1}UO₂PO₄·6H₂O has been prepared by precipitation from an aqueous H₃PO₄ solution containing UO₂²⁺ and Cr(NH₃)₆³⁺ ions. An X-ray powder pattern of the solid shows a single phase which indexes in tetragonal symmetry with an interlamellar spacing of ~9.10 Å. Absorption and photoluminescence (PL) spectra of the compound are a superposition of UO₂²⁺ and Cr(NH₃)₆³⁺ bands. Excitation spectra and radiative quantum yields indicate that the excited host UO₂²⁺ chromophore transfers energy to the Cr(III) complex with nearly unit efficiency. Prolonged visible photolysis of the solid at 295 K yields Cr(NH₃)(H₂O)₅³⁺ and Cr(NH₃)₂(H₂O)₄³⁺ as the principal products. Lower limit quantum yields for the initial appearance of interlamellar NH₄⁺ and NH₃, measured by IR spectroscopy, are ~0.1 with excitation of either the UO₂²⁺ or Cr(NH₃)₆³⁺ chromophore, demonstrating that ligand photosubstitution in a lamellar solid can be very efficient.

Intercalation chemistry¹ and solid-state photoprocesses² have been the subjects of intense investigation. Despite the substantial interest in these two areas, relatively few studies have explored their common ground, the excited-state properties of lamellar solids. We recently reported on the emissive properties of the layered compound hydrogen uranyl phosphate (HUP), HUO₂P·O₄·4H₂O, and of solids derived therefrom by cationic substitution.³ The substantial quenching of uranyl emission observed with Ag⁺, Cu²⁺, and *n*-C₄H₉NH₃⁺ prompted us to prepare HUP derivatives

wherein host–guest, excited-state interactions might be more directly probed.

We report in this paper on the excited-state properties of Cr(NH₃)₆³⁺-substituted HUP. Specifically, we demonstrate that this solid exhibits photoluminescence (PL) and photoreactivity characteristic of the Cr(III) complex upon excitation of either the guest Cr(III) or host UO₂²⁺ chromophore. Besides providing evidence for energy transfer, this system demonstrates that efficient ligand photosubstitution can obtain in a layered solid and, more generally, illustrates the ability of lamellar solids to serve as novel media for studying excited-state processes.

Results and Discussion

The introduction of a wide variety of mono- and divalent cations into the lamellar HUP lattice by intercalative ion-exchange reactions^{3,4} suggested to us that the host lattice might also be amenable to the incorporation of trivalent cations. With its well-characterized solution PL and photoreactivity, Cr(NH₃)₆³⁺

(1) For a recent overview, see: "Intercalation Chemistry"; Whittingham, M. S., Jacobson, A. J. Eds.; Academic Press: New York, 1982.

(2) For reviews involving solid-state photochemistry of transition-metal complexes relevant to this study, see, for example: (a) Simmons, E. L.; Wendlandt, W. W. *Coord. Chem. Rev.* **1971**, *7*, 11–27. (b) Fleischauer, P. D. In "Concepts of Inorganic Photochemistry"; Adamson, A. W., Fleischauer, P. D., Eds.; Wiley-Interscience: New York, 1975; Chapter 9. For reviews involving solid-state energy transfer, see, for example: (a) Reisfeld, R. *Struct. Bonding (Berlin)* **1976**, *30*, 65–97. (b) Reisfeld, R.; Jørgensen, C. K. *Ibid.* **1982**, *49*, 1–36.

(3) Olken, M. M.; Biagioni, R. N.; Ellis, A. B. *Inorg. Chem.* **1983**, *22*, 4128–34.

(4) Weigel, F.; Hoffmann, G. *J. Less-Common Met.* **1976**, *44*, 99–123.